

## Structural, electronic and magnetic properties of new full Heusler alloys $Rh_2CrZ$ ( $Z = Al, Ga, In$ ): First-principles calculations



L. Boumia<sup>a</sup>, F. Dahmane<sup>a,b,\*</sup>, B. Doumi<sup>c</sup>, D.P. Rai<sup>d</sup>, Shakeel A. Khandy<sup>e</sup>, H. Khachai<sup>f</sup>, H. Meradji<sup>g</sup>, Ali H. Reshak<sup>h,i,j,k</sup>, R. Khenata<sup>b</sup>

<sup>a</sup> Département de SM, Institut des Sciences et des Technologies, Centre Universitaire de Tissemsilt, Tissemsilt 38000, Algeria

<sup>b</sup> Laboratoire de Physique Quantique et de Modélisation Mathématique (LPQ3M), Département de Technologie, Université de Mascara, Mascara 29000, Algeria

<sup>c</sup> Faculty of Sciences, Department of Physics, Dr. Tahar Moulay University of Saida, Saida 20000, Algeria

<sup>d</sup> Department of Physics, Pachhunga University College, Aizawl 796001, India

<sup>e</sup> Department of Physics, Islamic University of Science and Technology, Awantipora, Jammu and Kashmir 192122, India

<sup>f</sup> Laboratoire d'étude des Matériaux & Instrumentations Optiques, Physics Department, Djillali Liabès University of Sidi Bel-Abbès, Sidi Bel-Abbès 22000, Algeria

<sup>g</sup> Laboratoire de Physique des Rayonnements, Département de Physique, Faculté des Sciences, Université Badji Mokhtar, Annaba, Algeria

<sup>h</sup> Department of Instrumentation and Control Engineering, Faculty of Mechanical Engineering, CTU in Prague, Technická 4, Prague 6 166 07, Czech Republic

<sup>i</sup> Nanotechnology and Catalysis Research Center (NANOCAT), University of Malaya, Kuala Lumpur 50603, Malaysia

<sup>j</sup> Physics department, College of Science, Basrah University, Basrah, Iraq

<sup>k</sup> Iraq University College (IUC), Al-Estiqal St., Basrah, Iraq

### ARTICLE INFO

#### Keywords:

First-principles calculations  
Heusler alloys  
Structural properties  
Magnetic properties  
Half metallicity

### ABSTRACT

First-principles calculations based on the density functional theory (DFT) within full-potential linearized augmented plane wave method (FP-LAPW) were carried out to investigate the structural, electronic and magnetic properties of  $Rh_2CrZ$  ( $Z = Al, Ga, In$ ) Heusler alloys. The electron exchange-correlation energy is described by the generalized gradient approximation (GGA-PBE), Tran and Blaha modified Becke-Johnson (TB-mBJ) potential and GGA + U (U is Hubbard correction). The present work reveals the stability of  $Rh_2CrZ$  ( $Z = Al, Ga, In$ ) Heusler in  $Cu_2MnAl$ -type structure. The negative value of formation energy in  $Rh_2CrZ$  ( $Z = Al, Ga, In$ ) alloys indicates that these compounds can be synthesized experimentally.  $Rh_2CrZ$  ( $Z = Al, Ga$ ) are half metal ferromagnets and expected to be potential candidates for application in spintronics. However,  $Rh_2CrIn$  is nearly half metallic behavior.

### 1. Introduction

Half-metallic (HM) materials are considered to be the most promising one, characterized by a metallic behavior in one spin channel and semiconducting nature for the other leads to 100% spin polarization at the Fermi level. The HM materials are the key in terms of technological importance and a prospective component of spintronic devices, in particular, as a resource of spin-injection into semiconductor substrates. Spintronic is a new form of electronics which utilizes the spin degree of freedom of electrons as well as

\* Corresponding author at: Département de SM, Institut des Sciences et des Technologies, Centre Universitaire de Tissemsilt, Tissemsilt 38000, Algeria.

E-mail address: [fethallah05@gmail.com](mailto:fethallah05@gmail.com) (F. Dahmane).

<https://doi.org/10.1016/j.cjph.2019.04.002>

Received 7 December 2018; Received in revised form 20 March 2019; Accepted 1 April 2019

Available online 10 April 2019

0577-9073/ © 2019 The Physical Society of the Republic of China (Taiwan). Published by Elsevier B.V. All rights reserved.

their charge [1]. While the concept of the half-metal was first originated from the electronic structure calculations in half-Heusler NiMnSb by de Groot et al. in 1983 [2]. This material opens an opportunity for innovation of devices joining standard microelectronic with spin-dependent effects such as nonvolatile magnetic random access memories and magnetic sensors [3]. In the recent years, half-metallic ferromagnetism has been investigated in several transition metal compounds such as 3d (V, Cr, and Mn)-doped GaP [4],  $\text{Be}_{1-x}\text{V}_x\text{Z}$  (Z = S, Se and Te) ( $x = 0.25$ ) [5]  $\text{Ti}_2\text{ZAl}$  (Z = Co, Fe, Mn) [6],  $\text{Co}_2\text{CrX}$  (X = Al, Ga, In) [7],  $\text{Co}_2\text{MnZ}$  (Z = Al, Ge, Si, Ga) [8],  $\text{ZnCdTMn}$  (T = Fe, Ru, Os, Rh, Ir, Ni, Pd, Pt) [9],  $\text{NbCoCrAl}$  and  $\text{NbRhCrAl}$  [10],  $\text{TaCoSn}$  [11],  $\text{Mn}_2\text{ZrX}$  (X = Ge, Si) [12], 171 Scandium-based full Heusler compounds [13], spin-gapless semiconductors  $\text{CuMn}_2\text{InSe}_4$  [14].

Heusler alloys [15], are potential materials with diverse applications in spintronic devices such as spin-resonant tunneling diodes, spintronic transistors, and spin light-emitting diodes etc. [16]. These materials can be used as spin injectors for magnetic random-access memories and other spin-dependent devices [17]. Half-metallic Heusler alloys are expected to play a key role in spintronic applications due to their high Curie temperatures and their structural compatibility with the widely used binary semiconductors crystallizing in the zinc-blende structure, such as GaN and GaAs, which are the most important materials to study both theoretical and experimental projects [17,18]. The greater part of these alloys forms  $L_{21}$  type crystal structures with a face-centered cubic lattice (fcc).

It was shown that the change of the main group element in Heusler alloys is a powerful tool to change their physical properties [19]. For example, electron spins polarization of full-Heusler alloy  $\text{Fe}_2\text{MnGe}$  is 96%, but replacing of Ge by Al, leads to a decrease of polarization to 81% [19].

The objective of this research work is to study the structural, electronic, magnetic and half-metallic behavior of the Heusler alloys  $\text{Rh}_2\text{CrZ}$  (Z = Al, Ga, In) with ab initio calculations. The rest of the paper is arranged as follows: Section 2 includes computational details and the method of calculation, Section 3 is devoted to the results and their discussions and Section 4 is a summary of our conclusions.

## 2. Computational details

The structural, electronic and magnetic properties of  $\text{Rh}_2\text{CrZ}$  (Z = Al, Ga, In) Heusler alloys are studied by using the full-potential linearized augmented plane-wave (FP-LAPW) method implemented in WIEN2k code [20]. The electronic exchange and correlation effects were performed with the generalized gradient approximation (GGA) of Perdew–Burke and Ernzerhof (PBE) [21]. In addition, Tran and Blaha modified Becke–Johnson (TB-mBJ) potential is also used to predict the band gap more specifically [22]. In order to study the on-site correlation at the 3d transition metals, the GGA + U method were used. In the GGA + U scheme, the effective Coulomb-exchange parameter  $U_{\text{eff}} = U - J$  should be used where U is the Coulomb part (Hubbard U) and J is the exchange part. We have chosen  $U = 1.64$  eV and  $J = 0.0$  eV for Cr.

In FP-LAPW method the space is divided into an interstitial region (IR) and non-overlapping muffin-tin (MT) spheres centered at the atomic sites. In the IR region, the basis set consists of plane waves. Inside the MT spheres, the basic functions are expanded into spherical harmonic functions. The wave functions in the interstitial region were expanded in plane waves with a cut-off  $K_{\text{max}} = 8/R_{\text{MT}}$ , where  $R_{\text{MT}}$  denotes the smallest atomic sphere radius and  $K_{\text{max}}$  is the maximum modulus for the reciprocal lattice vectors. The convergence criterion for self-consistent calculations was set to less than 0.1 mRy for energy. The cut-off energy, which defines the separation of valence and core states, was taken to be -6.0 Ry. The magnitude of the largest vector in charge density Fourier expansion ( $G_{\text{max}}$ ) was  $14$  (a.u.)<sup>-1</sup>. A mesh of 64 special  $k$ -points was made in the irreducible wedge of the Brillouin zone. In all calculations, the Rh:  $[\text{Kr}] 5s^1 4d^8$ , Cr:  $[\text{Ar}] 4s^1 3d^5$ , Ga:  $[\text{Ar}] 4s^2 3d^{10} 4p^1$ , Al:  $[\text{Ne}] 3s^2 3p^1$ , In:  $[\text{Kr}] 5s^2 4d^{10} 5p^1$  states are treated as valence electrons. In the goal to determine the ground-state properties the total energy dependence on the cell volume is fitted to the Murnaghan's equation of state [23] given by the following relation.

$$E = E_0(V) + \frac{BV}{B'(B' - 1)} \left[ B \left( 1 - \frac{V_0}{V} \right) + \left( \frac{V_0}{V} \right)^{B'} - 1 \right] \quad (1)$$

where  $E_0$  is the minimum energy at  $T = 0$  K,  $B$  is the bulk modulus,  $B'$  is the bulk modulus derivative and  $V_0$  is the equilibrium volume.

## 3. Results and discussions

### 3.1. Structural and elastic properties

Full-Heusler compounds with general chemical formula  $X_2YZ$ , where X and Y are transition metals and Z is a main group metal have face-centered cubic lattice (fcc) with space group Fm3m. These alloys are divided into two distinct groups due to their crystalline structures. The first type is with  $\text{Cu}_2\text{MnAl}$  ( $L_{21}$ ) structure, where the X atoms occupy (0, 0, 0) and (0.5, 0.5, 0.5) positions, Y atom occupies (0.25, 0.25, 0.25) position, and Z atom occupies (0.75, 0.75, 0.75) position. The  $X_2$  atoms form a primitive cubic sublattice while the adjacent cubes of this sublattice are filled alternately by Y or Z atoms [24]. The second type so-called inverse Heusler alloy is with XA-structure (prototype  $\text{Hg}_2\text{CuTi}$ ) where X atoms are positioned at (0, 0, 0) and (0.25, 0.25, 0.5) sites, the Y and Z atoms are at (0.5, 0.5, 0.5) and (0.75, 0.75, 0.75) sites, respectively. The crystal structure of  $\text{Rh}_2\text{CrZ}$  (Z = Al, Ga, In) in both  $\text{Hg}_2\text{CuTi}$  and  $\text{Cu}_2\text{MnAl}$  phases are shown in (Fig. 1).

In  $X_2YZ$  compounds, the site favorite of X and Y atoms are mostly determined by the number of their valence electrons, and when the number of 3d valence electrons of Y atom is larger than that of X in full-Heusler alloy, the inverse Heusler structure ( $\text{Hg}_2\text{CuTi}$ -

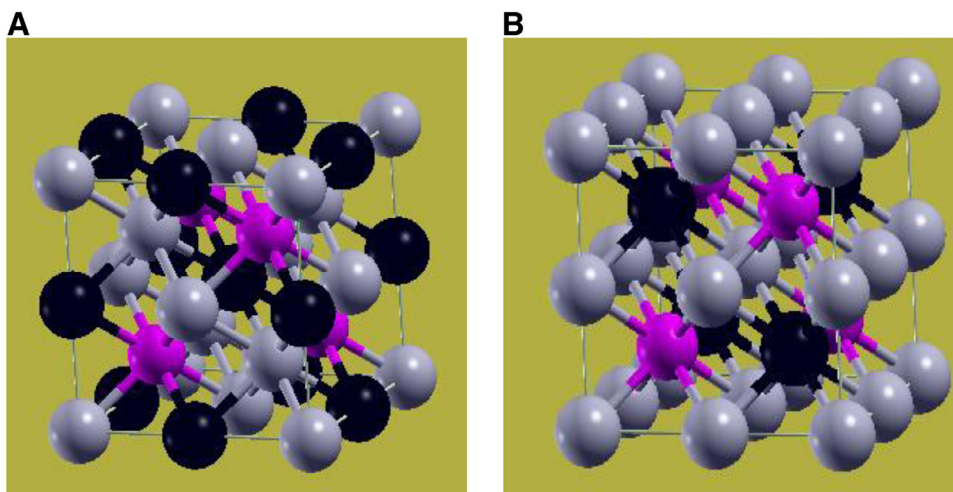


Fig. 1. Crystal structure of  $Rh_2CrZ$  ( $Z = Al, Ga, In$ ): (A)  $Hg_2CuTi$ , and (B)  $Cu_2MnAl$ : Rh (grey), Cr (black) and Z (purple).

type) will be observed. In order to predict the ground state properties and to establish the more stable structure for the  $Rh_2CrZ$  ( $Z = Al, Ga, In$ ) alloys, we have used the energy minimization method. Our basic procedure in this method, is to calculate the total energy as a function of unit-cell volume around the equilibrium state volume in both type phases  $Cu_2MnAl$  and  $Hg_2CuTi$  for the different volumes around the equilibrium cell volume  $V_0$  and by fitting the modified Birch-Murnaghan equation of state (EOS) [23].

In the case of  $Rh_2CrZ$  ( $Z = Al, Ga, In$ ), the Y (Cr) atomic number is 24 lower than the X (Rh) atomic number of 45; consequently,  $Cu_2MnAl$  type as a prototype is observed. In Fig. 2 we have compared the structural stability of  $Rh_2CrZ$  ( $Z = Al, Ga, In$ ) with  $Cu_2MnAl$  type and  $Hg_2CuTi$  type of structures, it is seen that the  $Cu_2MnAl$ -type phase is more stable than that of  $Hg_2CuTi$  phase for the  $Rh_2CrZ$  ( $Z = Al, Ga, In$ ) compounds at ambient conditions. The calculated ground-state parameters ( $a_0$ , B, B', V and  $E_0$ ) for the compounds are listed in Table 1.

The equilibrium lattice constants are found to be equal to 6.04 Å (6.06 Å), 6.10 Å (6.09 Å) and 6.32 Å (6.29 Å) for  $Rh_2CrAl$ ,  $Rh_2CrGa$  and  $Rh_2CrIn$ , respectively with  $Hg_2CuTi$  ( $Cu_2MnAl$ ) type structure. The equilibrium lattice constants of  $Rh_2CrZ$  ( $Z = Al, Ga, In$ ) increases with increasing in the covalent radii of Z atoms.

We discuss the phase stability of  $Rh_2CrZ$  ( $Z = Al, Ga, In$ ) alloys based on the formation energies  $E_f$  (formation enthalpies at 0 K) calculation using density functional theory. This can facilitate to predict whether these alloys can be fabricated experimentally or not. The formation energy ( $E_f$ ) shows the stability of the compound which is defined by the following equation for the  $Rh_2CrZ$  ( $Z = Al, Ga, In$ ):

$$E_f = E_{Rh_2CrZ}^{total} - [2E_{Rh}^{bulk} + E_{Cr}^{bulk} + E_{Al}^{bulk}] \quad (2)$$

where  $E_{Rh_2CrZ}^{total}$  is the calculated equilibrium total energy of the  $Rh_2CrZ$  ( $Z = Al, Ga, In$ ) compounds per formula unit and  $E_{Rh}^{bulk}$ ,  $E_{Cr}^{bulk}$ ,  $E_{Al}^{bulk}$  correspond to the total energy per atom for the Rh, Cr, and Al atoms, respectively. The calculated formation energies are shown in Table 1.

The negative value of formation energies indicates that the  $Rh_2CrZ$  ( $Z = Al, Ga, In$ ) compounds are energetically stable and their

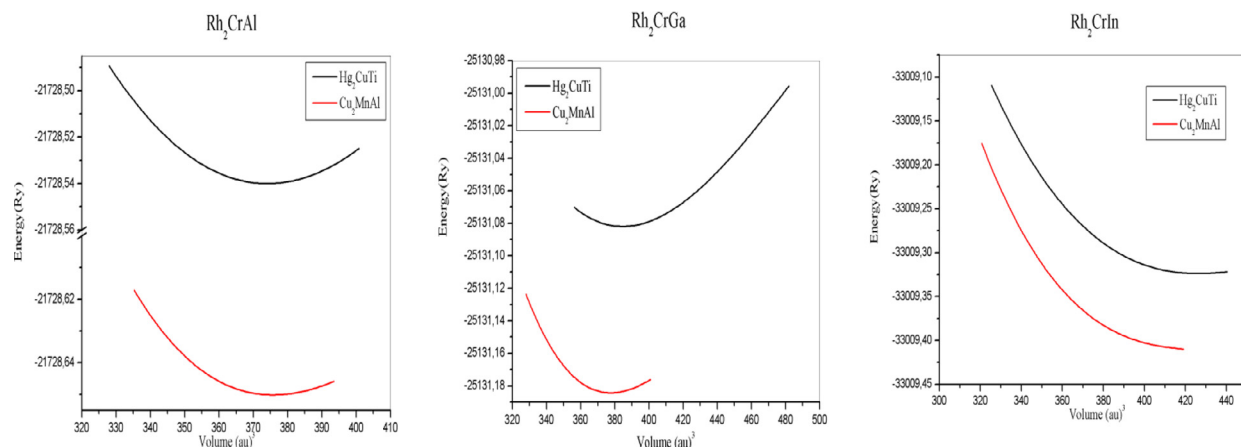


Fig. 2. Total energy as a function of unit cell volume for the  $Rh_2CrZ$  ( $Z = Al, Ga, In$ ) compounds in both  $Cu_2MnAl$ - and  $Hg_2CuTi$ -type structures.

**Table 1**

The calculated bulk parameters of Rh<sub>2</sub>CrZ (Z = Al, Ga, In) compounds, a (Å): lattice parameter, B (GPa): bulk modulus, B': Pressure derivative of the bulk modulus.

|                      |                      | a (Å)      | B (GPa)     | B'        | V <sub>0</sub> (a.u.) <sup>3</sup> | E <sub>0</sub> (Ry) | E <sub>r</sub> (Ry) |
|----------------------|----------------------|------------|-------------|-----------|------------------------------------|---------------------|---------------------|
| Rh <sub>2</sub> CrAl | Hg <sub>2</sub> CuTi | 6.0475     | 228.4502    | 3.1733    | 373.1789                           | -21,728.539590      | -1.7135             |
|                      | Cu <sub>2</sub> MnAl | 6.04 [25]  | 167.9418    | 5.9164    | 375.9945                           | -21,728.650114      | -1.8241             |
| Rh <sub>2</sub> CrGa | Hg <sub>2</sub> CuTi | 6.1048     | 154.6070    | 4.8837    | 383.6446                           | -25,131.082042      | -1.5842             |
|                      | Cu <sub>2</sub> MnAl | 6.0984     | 156.9161    | 6.2043    | 383.0189                           | -25,131.186243      | -1.6883             |
| Rh <sub>2</sub> CrIn | Hg <sub>2</sub> CuTi | 6.3242     | 168.9794    | 3.7160    | 426.8480                           | -33,009.324194      | -1.4275             |
|                      | Cu <sub>2</sub> MnAl | 6.28 [25]  | 178.618     | 4.3567    | 419.3142                           | -33,009.409367      | -1.5127             |
| Rh <sub>2</sub> MnAl |                      | 6.282 [26] | 213.01 [27] | 4.30 [27] | -                                  | -21,940.52 [27]     |                     |
|                      |                      | 5.98 [27]  |             |           |                                    |                     |                     |

experimental synthetization is realistic.

The calculated values of the formation energy of the Cu<sub>2</sub>MnAl-type structure are more negative than those calculated for the Hg<sub>2</sub>CuTi-type structure, indicating that the Cu<sub>2</sub>MnAl-type structure is more stable than that of Hg<sub>2</sub>CuTi-type one.

The responses of a crystalline solid to external stress of various natures are completely determined by the elastic constants and moduli. These parameters are fundamental and are intimately related with the bonding strength and lattice stability of the compound [28]. As there are no experimental or theoretical data for the elastic constants of the title compounds in the literature therefore, it is valuable to evaluate these parameters. These constants are computed by using the numerical first principles method where the curvature of the energy curve as a function of strain were analyzed for selected deformations of the unit cell. As the Rh<sub>2</sub>CrM (M = Al, Ga, In) compounds have the cubic structure; hence, it is necessary to calculate only three-independent single elastic constants namely C<sub>11</sub>, C<sub>12</sub>, and C<sub>44</sub>. These are listed in Table 2. In view on Table 2, one can notice that, C<sub>11</sub>, which is related to the unidirectional compression along the principal crystallographic directions is much higher than C<sub>44</sub>, indicating that these compounds present a weaker resistance to the pure shear deformation compared to the resistance to the unidirectional compression. One can remark that these materials have high elastic moduli which indicate their stiffness and rigidity.

To confirm the mechanical stability of the cubic system, the following mechanical stability criteria were checked by using the following known relation:

$$(C_{11} - C_{12}) > 0, C_{12} < B < C_{11}, (C_{11} + 2C_{12}) > 0, C_{44} > 0. \tag{3}$$

In our case, all the C<sub>ij</sub> constants satisfied the mechanical stability criteria, so it can be said that both studied compounds are mechanically stable.

The polycrystalline elastic moduli of the considered compounds, such as the bulk modulus B, shear modulus G, Young's modulus E, Poisson's ratio ν, were calculated from the single-crystal elastic constants C<sub>ij</sub> approach using the Voigt–Reuss–Hill approximations [29,30]:

$$B = \frac{(C_{11} + 2C_{12})}{3} \tag{4}$$

$$G_v = \frac{(C_{11} - C_{12} + 3C_{44})}{5} \tag{5}$$

$$G_R = \frac{5C_{44} (C_{11} - C_{12})}{4C_{44} + 3 (C_{11} - C_{12})} \tag{6}$$

$$G = \frac{(G_v + G_R)}{2} \tag{7}$$

$$E = \frac{9BG}{(3B + G)} \tag{8}$$

**Table 2**

Calculated elastic constants C<sub>ij</sub> (in GPa), shear moduli G<sub>v</sub> and G<sub>R</sub> (in GPa), Young modulus E (in GPa), Poisson ratio (ν), anisotropy elastic A, and B/G ratio (where B is the bulk modulus in GPa) for Rh<sub>2</sub>CrM (M = Al, Ga, In) in Cu<sub>2</sub>MnAl structure using GGA-PBE approximation.

|                      | C <sub>11</sub> | C <sub>12</sub> | C <sub>44</sub> | G <sub>v</sub> | G <sub>R</sub> | G     | E      | ν    | A    | B/G  |
|----------------------|-----------------|-----------------|-----------------|----------------|----------------|-------|--------|------|------|------|
| Rh <sub>2</sub> CrAl | 188.91          | 162.46          | 49.32           | 34.88          | 23.58          | 29.23 | 82.97  | 0.42 | 0.73 | 5.86 |
| Rh <sub>2</sub> CrGa | 199.37          | 138.62          | 74.18           | 56.66          | 47.04          | 51.85 | 140.29 | 0.35 | 0.44 | 3.06 |
| Rh <sub>2</sub> CrIn | 254.42          | 104.78          | 92.98           | 85.72          | 84.75          | 85.23 | 216.02 | 0.27 | 0.24 | 1.81 |

$$\nu = \frac{3B - 2G}{2(3B + G)} \quad (9)$$

$$A = \frac{2C_{44}}{(C_{11} - C_{12})} \quad (10)$$

The calculated polycrystalline elastic moduli are also listed in Table 2. For the estimation of the brittle and ductile behaviors of polycrystalline materials, Pugh [31] formulated an empirical formula in which the bulk modulus  $B$  and the shear modulus  $G$  are considered as resistant to fracture and to plastic deformation, respectively. This formula states that the critical value of the  $B/G$  ratio separating the ductile and brittle behavior of materials is around 1.75; i.e., if  $B/G > 1.75$ , the material is ductile; otherwise the material is classified as brittle [32]. The obtained  $B/G$  ratios for all the studied compounds are greater than 1.75, indicating the ductile nature of these compounds. The ductile characteristic of these compounds is also confirmed by the Cauchy's pressure relation defined as the difference between the elastic constants  $C_{11} - C_{12}$ . If the Cauchy's pressure is positive (negative), the material is expected to be ductile (brittle) [33,34]. Here, the calculated Cauchy's pressure is positive for all compounds. Therefore, these compounds are classified as ductile materials. It is seen that the ductility increases in the following sequence:  $(\text{Rh}_2\text{CrIn}) < (\text{Rh}_2\text{CrGa}) < (\text{Rh}_2\text{CrAl})$  which implies that replacing metal "M" with another more electronegative metal leads to more ductile compound. The important quantity known as the Poisson ratio ( $\nu$ ) characterizes the bonding nature of solid materials where the Poisson ratio ( $\nu$ ) for covalent materials has a small value typically at 0.1 and for ionic compounds, its typical value is greater than or equal to 0.25. As the calculated ( $\nu$ ) value for  $\text{Rh}_2\text{CrM}$  ( $M = \text{Al}, \text{Ga}, \text{In}$ ) compounds are greater than 0.25, this indicates ionic bonding for these compounds. The elastic anisotropy ( $A$ ) is an important factor, as it is highly correlated with possibility of inducing microcracks in the materials. For completely isotropic systems, the anisotropy factor  $A$  takes the value of the unity and the deviation from unity measures the degree of elastic anisotropy. The calculated values of the anisotropic factor  $A$  are larger than the unity for all the investigated compounds, meaning that they are characterized by a profound anisotropy.

### 3.2. Electronic and magnetic properties

In order to predict the electronic properties of  $\text{Rh}_2\text{CrZ}$  ( $Z = \text{Al}, \text{Ga}, \text{In}$ ), we have presented the total density of states (TDOS) as a function of energy for  $\text{Rh}_2\text{CrZ}$  ( $Z = \text{Al}, \text{Ga}, \text{In}$ ) with  $\text{Hg}_2\text{CuTi}$  type structure (Fig. 3) and  $\text{Cu}_2\text{MnAl}$  (Fig. 4), by using GGA, TB-mBJ and GGA + U approximations. The Fermi level sets as 0.0 eV. The partial densities of states (PDOS) spectra are computed to see the contributions from various atomic states near  $E_F$ . The role of transition metals 3d-states is very important in the description of density of states calculations. The magnetic moments of the materials depend on the interactions of 3d-band structure with other states [35]. Coey et al. [36] have proposed a large classification scheme for half-metallic ferromagnets. A material with conducting electrons (metallic behavior) at one for the spin channels and an integer moment at  $T = 0$  is a good candidate for A type-I half-metallic ferromagnet. This is the phenomena described by de Groot et al. Type-I<sub>A</sub> half-metals are metallic in spin up, but semiconducting in spin dn; the opposite is true for the type-I<sub>B</sub> half-metals [37]. In  $\text{Hg}_2\text{CuTi}$  type structure, it is observed from Fig. 3 that the electronic structure has metallic intersections at the Fermi level, indicating a strong metallic nature of spin-up and spin-down electrons for  $\text{Rh}_2\text{CrZ}$  ( $Z = \text{Al}, \text{Ga}, \text{In}$ ) within GGA, TB-mBJ and GGA + U approximations. Fig. 4 also shows that the profile of the PDOS and TDOS spectra of the compounds of interest in the  $\text{Cu}_2\text{MnAl}$ -type structure is almost similar with  $Z$  ( $Z = \text{Al}, \text{Ga}$  and  $\text{In}$ ). It is clear that the majority-spin is metallic, while the minority spin shows a semiconducting gap around the Fermi level for  $\text{Rh}_2\text{CrZ}$  ( $Z = \text{Al}, \text{Ga},$ ) alloys. So,  $\text{Rh}_2\text{CrZ}$  ( $Z = \text{Al}, \text{Ga}$ ) compounds with  $\text{Cu}_2\text{MnAl}$  type structure are classified as a HM material. From the PDOS and TDOS, we can see the TDOS around the Fermi level comes mainly from the 4d electrons of transition metal. It is seen that the major contributions to the resulting density of states (DOS) of  $\text{Rh}_2\text{CrZ}$  ( $Z = \text{Al}, \text{Ga}, \text{In}$ ) obtained by both GGA and TB-mBJ approximations are due to the Rh atoms. For  $\text{Rh}_2\text{CrIn}$ , the PDOS and TDOS indicate nearly half-metallic behavior with small spin-down electronic densities of states at the Fermi level.

The minority-spin band gap is an important part in HM materials, and the source of the HM band gap is discussed in the following. The HM band gaps usually take place from three aspects [38]: (1) charge transfer band gap [38] which is frequently seen in  $\text{CrO}_2$  and double perovskites [38], covalent band gap which is present in the half- Heusler with  $C_{1b}$  structure, and (3) d-d band gap, that is the origin of the HM band gap in the full- Heusler alloys with  $\text{Cu}_2\text{MnAl}$  structure. Fig. 5 illustrate the hybridization between d-orbitals of Rh1(Rh2) and Cr atom. In the latter case there is a relatively strong hybridization between d orbitals of transition metals which makes the d-orbitals to split into bonding  $e_g$  and  $t_{2g}$  orbitals below the Fermi level and anti-bonding  $e_g^*$  and  $t_{2g}^*$  orbitals above the Fermi level. This hybridization is known as d-d hybridization [39].

The half- metallicity (HM) is one of the key ingredients for realization of spintronic devices because it is known to maximize the spin-injection rate of spin-polarized carriers into semiconductors [40].

The main group atom plays a central role to stabilize the half-metallicity, while it does not directly forms the minority gap, which provides p states to hybridize with d electrons and determines the degree of occupation of the p-d hybrids, thus affecting the formation of energy gap and the width of gap [41]. The half-metallic property of alloy is directly connected to its lattice constant due to the fact that the lattice constant significantly affects the width of the band-gap and the position of the Fermi level  $E_F$  relative to the band-gap as suggested by Qi and co-authors [42], Han et al. [43] and Wang and collaborators [44].  $\text{Rh}_2\text{CrAl}$  and  $\text{Rh}_2\text{CrGa}$  have HM behavior with lattice parameter 6.04 Å and 6.10 Å, respectively; this character begins to diminish with  $\text{Rh}_2\text{CrIn}$  with lattice parameter of 6.32 Å. Slater [45] and Pauling [46] separately establish that the magnetic moments per atom  $m$  of the 3d transition elements and their binary alloys can be predictable by the mean number of valence electrons per atom  $n_V$ .

Once we insert one valence electron in the compound, this resides in spin-down states only and the total spin magnetic moment

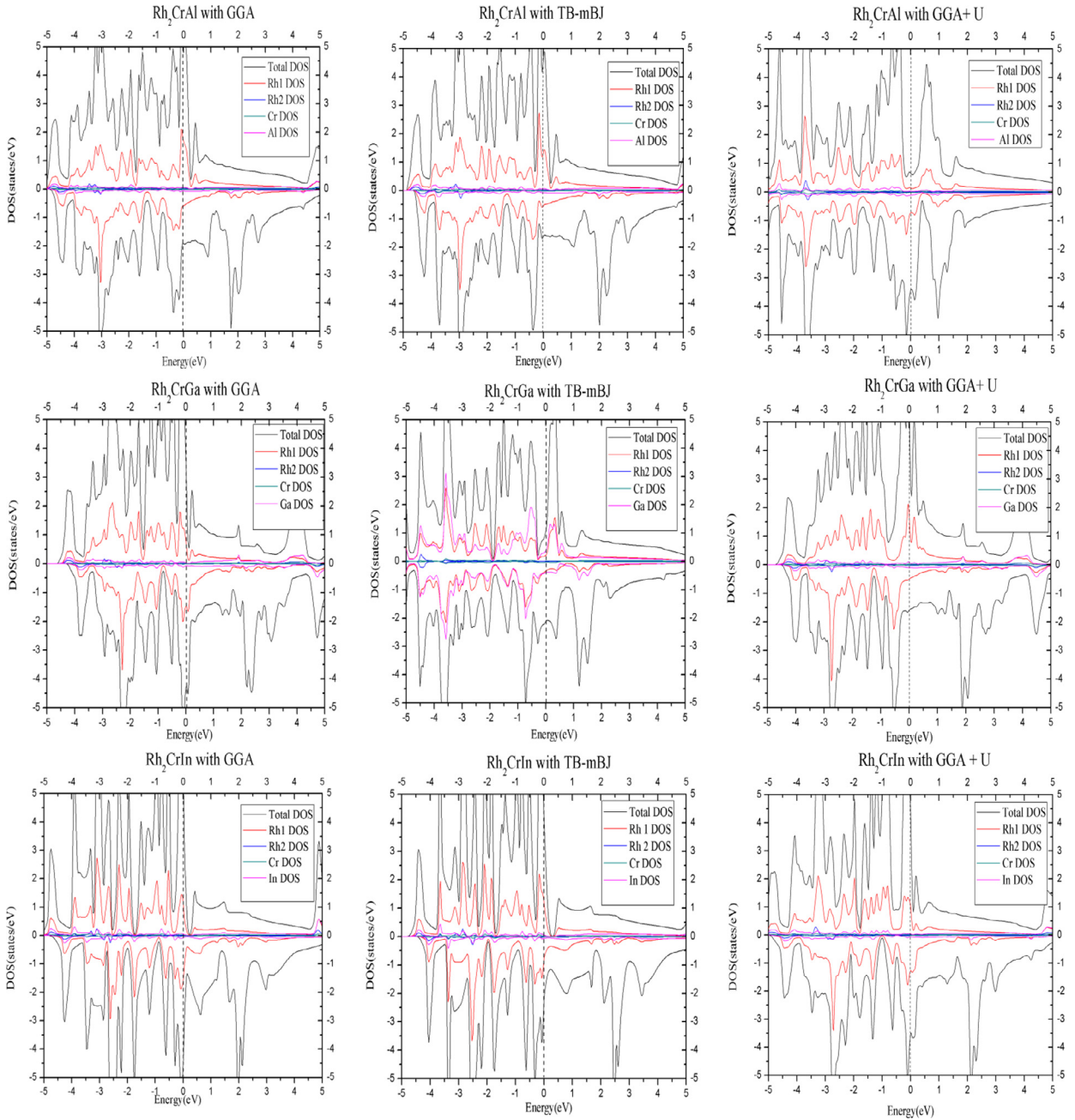


Fig. 3. DOS of Rh<sub>2</sub>CrZ (Z = Al, Ga, In) in Hg<sub>2</sub>CuTi type structure with GGA, TB-mBJ and GGA + U approximations.

decreases by about 1  $\mu_B$ . The Slater–Pauling rules connect the electronic properties directly to the magnetic properties (total spin magnetic moments) and thus present an influential tool to the study of half-metallic Heusler compounds. It was revealed that in the case of the semi-Heusler, the total spin magnetic moment in the unit cell,  $M_t$  scales as a function of the total number of valence electrons  $n_v$ , following the relation  $M_t = n_v - 18$  [47] whereas, in the case of the full Heusler alloys, this relation becomes  $M_t = n_v - 24$ . [48]. The number “24” in the above formula comes from number of completely occupied minority states which consist of one s, three p, and eight d states and gives total 12 states [48].

The total and partial magnetic moments, using GGA-PBE, TB-mBJ and GGA + U, of Rh<sub>2</sub>CrZ (Z = Al, Ga, In) with Cu<sub>2</sub>MnAl type structure (the most stable structure), are summarized Table 3. The values of  $M_t^{tot}$  obtained within GGA-PBE are slightly less than those calculated using GGA + U. The integer magnetic moment is a significant characteristic property for these systems in stoichiometric composition. The small deviation from integer magnetic moment guide significant disruptions in half-metallic character by non-zero electronic density of states for minority spins around Fermi level [49]. It is also an important question that in what conditions half-

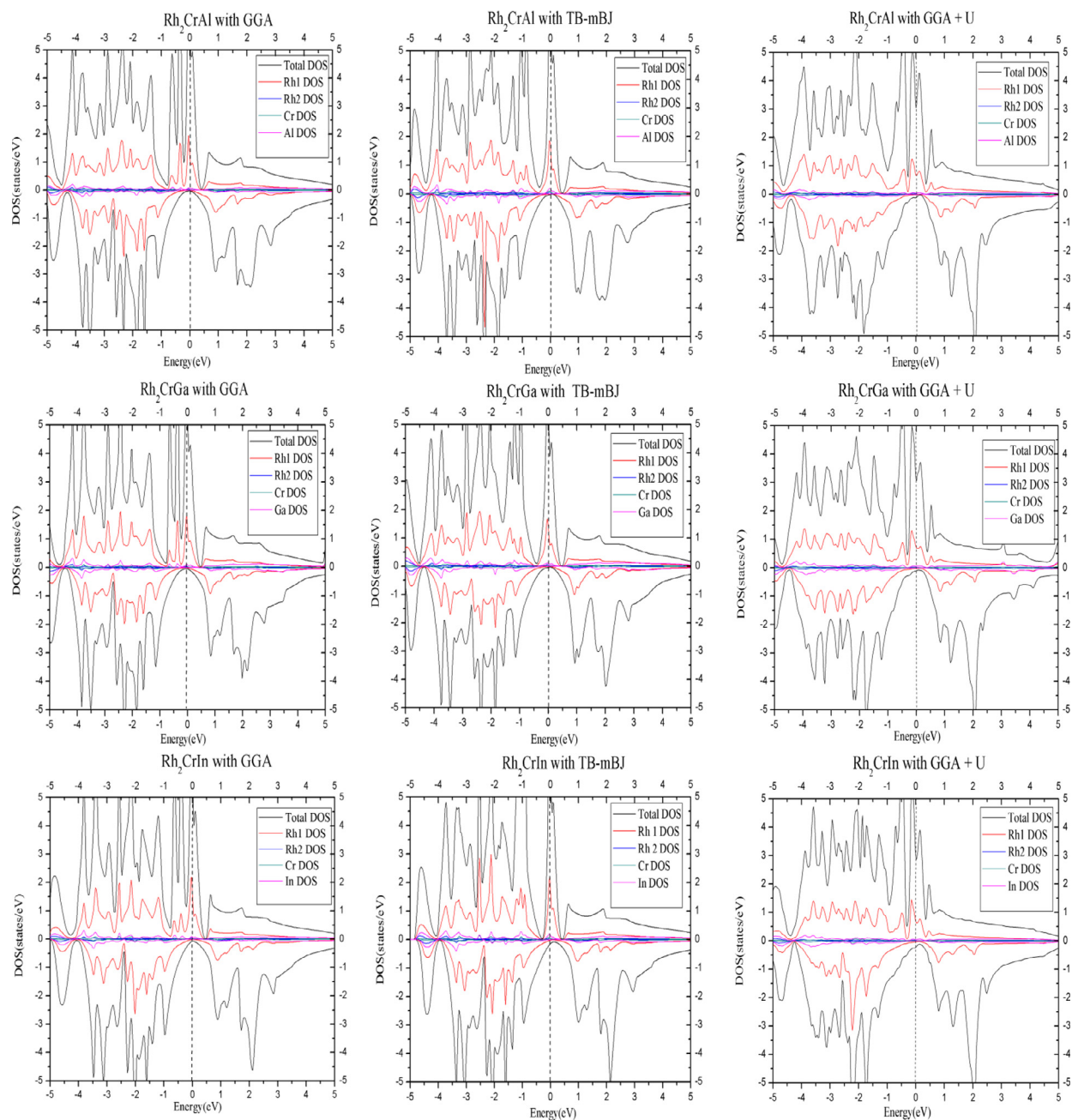


Fig. 4. DOS of  $\text{Rh}_2\text{CrZ}$  ( $Z = \text{Al, Ga, In}$ ) in  $\text{Cu}_2\text{MnAl}$  type structure with GGA, TB-mBJ and GGA + U approximations.

metallic character is preserved [49].

The calculated spin magnetic moments for the  $\text{Rh}_2\text{CrZ}$  ( $Z = \text{Al, Ga, In}$ ) Heusler alloys, expose that the total magnetic moments which contains the contribution from the  $\text{Rh}_1$ ,  $\text{Rh}_2$ , Cr, Z atoms and the interstitial region, comes mainly from the Cr ion, this contribution was due to the large exchange splitting between majority spin states and minority spin states of Cr atom, with a small contribution from Z ( $Z = \text{Al, Ga, In}$ ), Rh sites and interstitial region. The Z-element ( $Z = \text{Al, Ga, In}$ ) take a small magnetic moment which is owing to induced magnetic polarization by surrounding transition metal atoms. The negative sign in the local magnetic moments of Z atom shows that the induced magnetic polarization of the Z element is anti-parallel to that of Rh and Cr atoms. The  $\text{Rh}_2\text{CrZ}$  ( $Z = \text{Al, Ga, In}$ ) alloys have 27 valence electrons per unit cell ( $n_v = (9 \times 2) + 6 + 3 = 27$ ), consequently the spin magnetic moment  $M_t = 27 - 24 = 3$  in good agreement with the Slater Pauling rule  $M_t = n_v - 24$ .

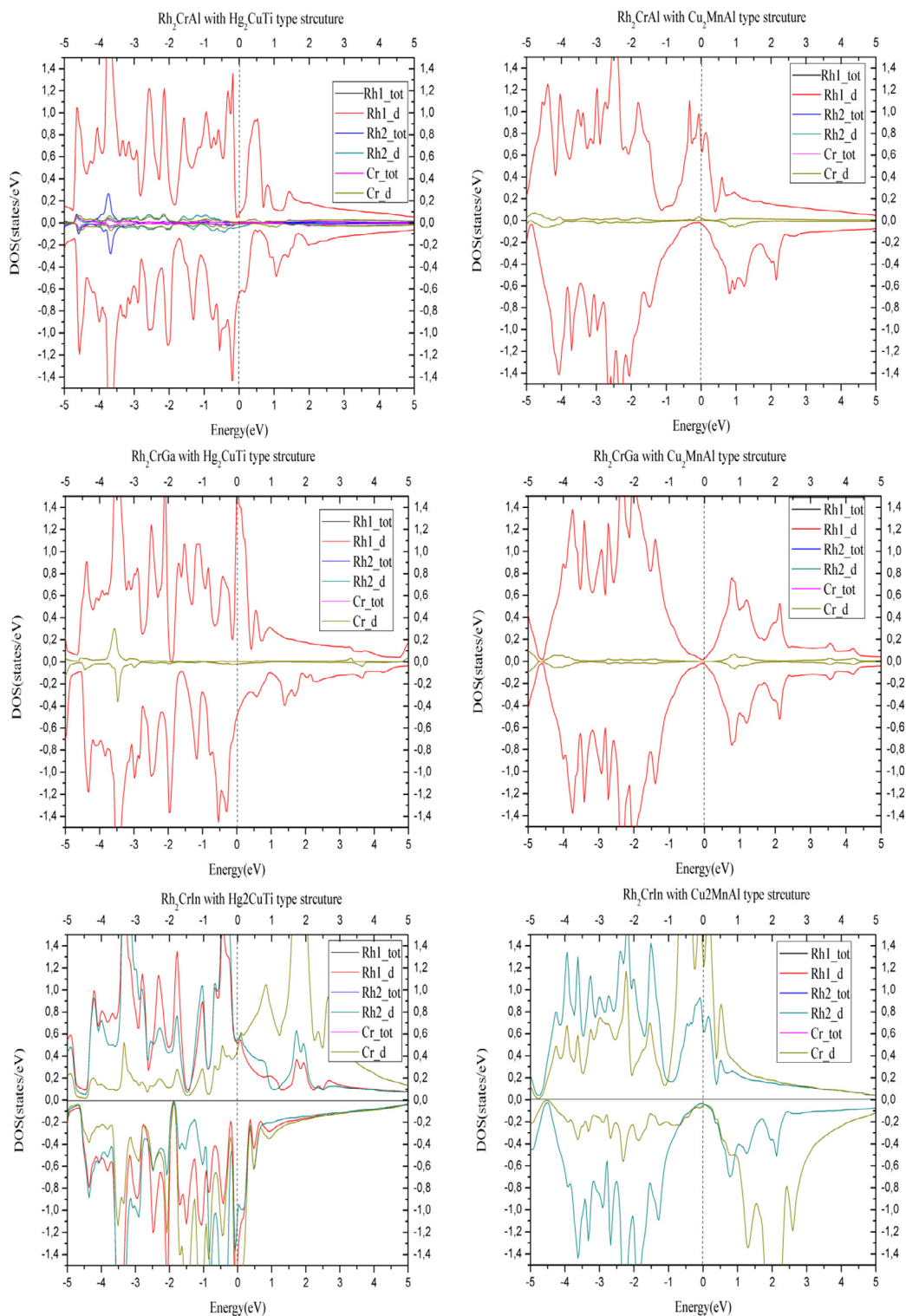


Fig. 5. PDOS of  $\text{Rh}_2\text{CrZ}$  ( $Z = \text{Al, Ga, In}$ ) in both  $\text{Cu}_2\text{MnAl}$  and  $\text{Hg}_2\text{CuTi}$  type structure.

#### 4. Conclusions

The structural, electronic and magnetic properties of the  $\text{Rh}_2\text{CrZ}$  ( $Z = \text{Al, Ga, In}$ ) for both  $\text{Hg}_2\text{CuTi}$  and  $\text{Cu}_2\text{MnAl}$  type structures have been investigated using first-principles calculations based on density functional theory (DFT).

**Table 3**The total and partial magnetic moments of Rh<sub>2</sub>CrZ (Z = Al, Ga, In).

|                      |         | M <sup>Rh1</sup> | M <sup>Rh2</sup> | M <sup>Cr</sup> | M <sup>Z</sup> | M <sup>interstitial</sup> | M <sup>total</sup> |
|----------------------|---------|------------------|------------------|-----------------|----------------|---------------------------|--------------------|
| Rh <sub>2</sub> CrAl | GGA     | 0.22267          | 0.15871          | 2.54878         | -0.02163       | 0.11542                   | 3.00396            |
|                      |         |                  |                  | 2.6 [26]        | 0.0 [26]       |                           | 3.01 [25]          |
|                      | TB-mBJ  | 0.28178          | 0.23958          | 2.55259         | -0.03995       | -0.03033                  | 3.000              |
| Rh <sub>2</sub> CrGa | GGA + U | 0.09777          | 0.42247          | 2.51888         | -0.03803       | -0.05052                  | 3.02161            |
|                      | GGA     | 0.16715          | 0.18356          | 2.54714         | -0.02214       | 0.13136                   | 3.00708            |
|                      | TB-mBJ  | 0.22972          | 0.23069          | 2.57435         | -0.03683       | 0.01405                   | 3.00198            |
| Rh <sub>2</sub> CrIn | GGA + U | 0.08819          | 0.39015          | 2.53750         | -0.03561       | 0.09402                   | 3.04426            |
|                      | GGA     | 0.15855          | 0.09881          | 2.64036         | -0.01691       | 0.15523                   | 3.03604            |
|                      | TB-mBJ  | 0.07270          | 0.08754          | 2.84591         | -0.01964       | 0.06533                   | 3.05185            |
| Rh <sub>2</sub> MnAl | GGA + U | 0.06087          | 0.34773          | 2.67977         | -0.02919       | 0.11039                   | 3.10958            |
|                      |         |                  |                  | 2.8 [26]        | 0.0 [26]       |                           | 3.14 [25]          |
|                      |         |                  |                  |                 |                |                           | 3.00 [26]          |
|                      |         |                  |                  |                 |                |                           | 3.05185            |
|                      |         |                  |                  |                 |                |                           | 3.10958            |
|                      |         |                  |                  |                 |                |                           | 4.04 [27]          |

- The Cu<sub>2</sub>MnAl-type phase is more stable than that of Hg<sub>2</sub>CuTi phase for Rh<sub>2</sub>CrZ (Z = Al, Ga, In) compounds at ambient conditions.
- Rh<sub>2</sub>CrZ (Z = Al, Ga) exhibits HM nature, Rh<sub>2</sub>CrIn displays a nearly half metallic behavior.
- The calculated total magnetic moments of 3 μ<sub>B</sub> for Rh<sub>2</sub>CrZ (Z = Al, Ga) are in good agreement with Slater Pauling rule, whereas that of 3.05 μ<sub>B</sub> for Rh<sub>2</sub>CrIn shows slight deviation from the Slater Pauling rule.

## References

- [1] L. Zhang, X.T. Wang, H. Rozale, Jian-Wei Lu, Li-ying Wang, J. Supercond. Nov. Magn. 29 (2016) 349–356.
- [2] R.A. de Groot, F.M. Mueller, P.G. van Engen, K.H.J. Buschow, Phys. Rev. Lett. 50 (1983) 2024.
- [3] Qing-Long Fang, Jian-Min Zhang, Ke-Wei Xu, J. Magn. Magn. Mater. 349 (2014) 104–108.
- [4] B. Doumi, A. Mokaddem, A. Sayede, M. Boutaleb, A. Tadjer, F. Dahmane, J. Supercond. Nov. Magn. 28 (2015) 3163.
- [5] B. Doumi, A. Mokaddem, A. Sayede, F. Dahmane, Y. Mogulkoc, A. Tadjer, Superlattices Microstruct. 88 (2015) 139.
- [6] F. Dahmane, S. Benalia, L. Djoudi, A. Tadjer, R. Khenata, B. Doumi, H. Aourag, J. Supercond. Nov. Magn. 28 (2015) 3099.
- [7] F. Dahmane, D. Mesri, A. Tadjer, R. Khenata, S. Benalia, L. Djoud, B. Doumi, L. Boumia, H. Aourag, Mod. Phys. Lett. B 30 (2016) 11 1550265.
- [8] F. Dahmane, B. Doumi, Y. Mogulkoc, A. Tadjer, Deo Prakash, K.D. Verma, Dinesh Varshney, M.A. Ghebouli, S. Bin Omran, R. Khenata, J. Supercond. Nov. Magn. 29 (2016) 809.
- [9] Yilin Han, Mengxin Wu, Minquan Kuang, Tie Yanga, Xuebin Chen, Xiaotian Wang, Results Phys. 11 (December) (2018) 1134–1141.
- [10] Y. Li, G.D. Liu, X.T. Wang, E.K. Liu, X.K. Xi, W.H. Wang, G.H. Wu, L.Y. Wang, X.F. Dai, Results Phys. 7 (2017) 2248–2254.
- [11] Enamul Haque, M. Anwar Hossain, Results Phys. 10 (September) (2018) 458–465.
- [12] Arash Anjami, Arash Boochani, Seyed Moahammad Elahi, Hossein Akbari, Results Phys. 7 (2017) 3522–3529.
- [13] Yilin Han, Zongbin Chen, Minquan Kuang, Zhuhong Liu, Xiangjian Wang, Xiaotian Wang, Results Phys. 12 (March) (2019) 435–446.
- [14] Yilin Han, R. Khenata, Tingzhou Li, Liying Wang, Xiaotian Wang, Results Phys. 10 (September) (2018) 301–303.
- [15] F. Heusler, Verh. Deutsch. Phys. Ges. 5 (1903) 219.
- [16] K. Seema, N.M. Umrans, R. Kumar, J. Supercond. Nov. Magn. 29 (2016) 401–408.
- [17] H. Zenasni, H.I. Farouq, C. Esling, J. Magn. Magn. Mater. 333 (2013) 162–168.
- [18] M. Khalifa, H. Khachai, F. Chiker, N. Baki, K. Bougherara, A. Yakoubi, G. Murtaza, M. Harmel, M.S. Abu-Jafar, S. Bin Omran, R. Khenata, Int. J. Mod. Phys. B 29 (2015) 1550229.
- [19] S.M. Azar, B.A. Hamad, J.M. Khalifeh, J. Magn. Magn. Mater. 324 (2012) 1776.
- [20] P. Blaha, K. Schwarz, G.K.H. Madsen, D. Kvasnicka, J. Luitz, WIEN2k, an Augmented Plane Wave Plus Local Orbitals Program for Calculating Crystal Properties, Vienna University of Technology, Vienna, 2001.
- [21] J.P. Perdew, K. Burke, M. Ernzerhof, Phys. Rev. Lett. 77 (1996) 3865.
- [22] F. Tran, P. Blaha, Phys. Rev. Lett. 102 (2009) 226401.
- [23] F.D. Murnaghan, Proc. Natl. Acad. Sci. USA 30 (1944) 5390.
- [24] V. Alijani, J. Winterlik, G.H. Fecher, S.S. Naghavi, S. Chadov, T. Gruhn, C. Felser, J. Phys. Condens. Matter 24 (2012) 7 046001.
- [25] M. Gilleßen, R. Dronskowski, J. Comput. Chem. 30 (2009) 1290–1299.
- [26] J. Balluff, Antiferromagnetic Heusler Compd. Spintronics (2017).
- [27] S. Berri, D. Maouche, M. Ibrir, F. Zerarga, L. Louail, Y. Medkour, Physica B 418 (2013) 58–64.
- [28] A. Bouhemadou, R. Khenata, M. Kharoubi, T. Seddik, A.H. Reshak, Y. Al-Douri, Comput. Mater. Sci. 38 (2006) 263.
- [29] W. Voigt, Lehrb. Der Krist. Leipzig (1928).
- [30] A. Reuss, Zeitschrift Angew. Math. Mech. 9 (1929) 49–58.
- [31] S.F. Pugh, Philos. Mag. Ser. 7 (45) (1954) 823.
- [32] S. Labidi, M. Labidi, F.E.H. Hassan, Sci. Lett. J. 1 (2012) 3.
- [33] V. Kanchana, G. Vaitheeswaran, Yanning Ma, Yu Xie, A. Svane, O. Eriksson, Phys. Rev. B 80 (2009) 125108.
- [34] F. Semari, R. Khenata, M. Rabah, A. Bouhemadou, S. Bin Omran, Ali H. Reshak, D. Rached, J. Solid State Chem. 183 (2010) 2818–2825.
- [35] S. Rauf, S. Arif, M. Haneef, Bin Amin, J. Phys. Chem. Solids 76 (2015) 153–169.
- [36] J.M.D. Coey, M. Venkatesan, M.A. Bari in Lecture Notes in Physics 595 Springer, Heidelberg, 2002, p. 377.
- [37] C. Felser, G.H. Fecher, B. Balke, Angew. Chem. Int. Ed. 46 (2007) 668–699.
- [38] F. Ahmadian, J. Alloys Compd. 576 (2013) 279–284.
- [39] S. Esteki, F. Ahmadian, J. Magn. Magn. Mater. 438 (2017) 12–19.
- [40] M. Kim, Jae Il Lee, J. Korean Phys. Soc. 60 (7) (2012) 1068–1071.
- [41] Ying Chen, Bo Wu, Hongkuan Yuan, Yu Feng, Hong Chen, J. Solid State Chem. 221 (2015) 311–317.
- [42] Santao Qi, Jiang Shen, Chuan-Hui Zhang, Mater. Chem. Phys. 164 (2015) 177–182.
- [43] Yilin Han, A. Bouhemadou, R. Khenata, Zhenxian Cheng, Tie Yang, Xiaotian Wang, J. Magn. Magn. Mater. 471 (2019) 49–55.
- [44] Xiaotian Wang, Weiqi Zhao, Zhenxiang Cheng, Xuefang Dai, R. Khenata, Solid State Commun. 269 (2018) 125–130.

- [45] J.C Slater, Phys. Rev. 49 (1936) 931–937.
- [46] L Pauling, Phys. Rev. 54 (1938) 899–904.
- [47] I. Galanakis, P.H. Dederichs, N. Papanikolaou, Phys. Rev. B 66 (2002) 134428.
- [48] I. Galanakis, P.H. Dederichs, N. Papanikolaou, Phys. Rev. B 66 (2002) 174429.
- [49] G Gökoğlu, O Gülseren, Eur. Phys. J. B 76 (2010) 321–326.